NEURODEVELOPMENT

Evolution of pallium, hippocampus, and cortical cell types revealed by single-cell transcriptomics in reptiles

Maria Antonietta Tosches,*† Tracy M. Yamawaki,*‡ Robert K. Naumann,§ Ariel A. Jacobi,‖ Georgi Tushev, Gilles Laurent†

Computations in the mammalian cortex are carried out by glutamatergic and γ-aminobutyric acid–releasing (GABAergic) neurons forming specialized circuits and areas. Here we asked how these neurons and areas evolved in amniotes. We built a gene expression atlas of the pallium of two reptilian species using large-scale single-cell messenger RNA sequencing. The transcriptomic signature of glutamatergic neurons in reptilian cortex suggests that mammalian neocortical layers are made of new cell types generated by diversification of ancestral gene-regulatory programs. By contrast, the diversity of reptilian cortical GABAergic neurons indicates that the interneuron classes known in mammals already existed in the common ancestor of all amniotes.

Amniote vertebrates (mammals, reptiles, and birds) originated from a common ancestor about 320 million years ago. In all developing amniotes, the dorsal telencephalon, or pallium, is patterned by the same signaling molecules and subdivided in homologous embryonic regions (*1*). In adult amniote brains, however, the structures that arise from these homologous pallial regions have different morphologies and connectivity. For example, a six-layered neocortex exists only in mammals, and the dorsal ventricular ridge (DVR) is found only in birds and reptiles. The hippocampus may be the most conserved pallial region (*2*), but even there, it is uncertain whether all the subfields known in mammals (for example, the dentate gyrus) exist in nonmammals (*3*) (fig. S1).

Gene expression data can help reconstruct the evolution of brain regions and cell types (*4*, *5*). Here we used single-cell transcriptomics to study the evolution of neuronal diversity in the amniote telencephalon. Because cell types defined through transcriptomics match those defined by morphology, physiology, and connectivity (*6*–*8*), single-cell mRNA sequencing can be applied both for cell-type discovery and for cross-species comparisons (*9*). We focused on reptiles, because they, unlike birds, have a layered cortex, and asked the following: (i) Can we identify molecular similarities and homologies between reptilian and mammalian pallial regions? (ii) Are there reptilian cortical neurons homologous to mammalian hippocampal neurons? (iii) Can we link the reptilian three-layered cortex to the mammalian six-layered neocortex? (iv) Are mammalian γ-aminobutyric acid–releasing (GABAergic) interneuron types also found in the reptilian cortex?

Max Planck Institute for Brain Research, Max-von-Laue Strasse 4, 60438 Frankfurt am Main, Germany.
*These authors contributed equally to this work.
†Corresponding author. Email: gilles.laurent@brain.mpg.de (G.L.); maria.tosches@brain.mpg.de (M.A.T.) ‡Present address: Amgen, Inc., 1120 Veterans Blvd., South San Francisco, CA 94080, USA. §Present address: Shenzhen Institutes of Advanced Technology, Chinese Academy of Sciences, 1068 Xueyuan Ave., Shenzhen University Town, Nanshan District, 518055 Shenzhen, China. ‖Present address: University of California, Davis, School of Medicine, 4610 X St., Sacramento, CA 95817, USA.

Neuronal and glial cells in the reptilian pallium

Using Drop-seq (*8*), we obtained a comprehensive, unbiased classification of adult cell types sampled from the pallium of a turtle and a lizard species (dissections and sequencing statistics in figs. S1 and S2 and tables S1 and S2). After quality filtering (fig. S3), we used unsupervised graph-based clustering of the transcripts from 18,828 turtle and 4187 lizard cells (with a median of 2731.5 and 1918 transcripts per cell, respectively) and identified first-level clusters of neuronal and non-neuronal cells (Fig. 1, A to C). Among non-neuronal cells, we found clusters expressing prototypical markers of mammalian glial cells: mature oligodendrocytes and their precursors, ependymoglial cells, and microglia (Fig. 1, B to D). Ependymoglial cells coexpressed markers of mammalian astrocytes (*GFAP*), adult stem cells (*SOX9*), and ependymal cells (*FOXJ1*), suggesting a shared evolutionary origin of these cell types (fig. S4, A to C). Reptilian neuronal clusters included vesicular glutamate transporter type 1 (*VGLUT1*$^+$) glutamatergic excitatory neurons, glutamate decarboxylase 1 and 2 (*GAD1*$^+$ *GAD2*$^+$) GABAergic inhibitory interneurons, and neural progenitor cells (Fig. 1, A to D), consistent with the existence of adult neurogenesis in reptiles. To compare the transcriptomes of turtle, lizard, and mouse neuronal and non-neuronal cells (*6*), we selected one-to-one orthologs differentially expressed among these cell types, defined a specificity score for each gene in each cluster, and computed pairwise rank correlations (see methods). This analysis supports correspondence between major neuronal and non-neuronal cell classes (fig. S4, D to F) across turtle, lizard, and mouse.

Subclustering of the turtle and lizard neurons revealed finer distinctions between and within excitatory glutamatergic and inhibitory GABAergic neuron types (Fig. 1, E to G, and fig. S5). From these neuronal data sets, we selected differentially expressed genes as markers for histological validation and for unbiased comparisons with mammalian cell types. We focused on the turtle data and used the lizard data for corroboration.

Spatial segregation of glutamatergic neurons: A molecular map of the reptilian pallium

Our dissections encompassed multiple regions of the reptilian pallium likely to contain heterogeneous populations of glutamatergic neurons. To establish the anatomical location of our turtle glutamatergic-cell clusters, we selected highly variable genes in the data set that were expressed in some clusters but not detected in others. These markers were expressed in distinct regions of the pallium (fig. S6). The combinatorial expression of markers defined "superclusters," seen also as groupings of adjacent clusters in t-distributed stochastic neighbor embedding (tSNE) plots (Fig. 2, A to B, and fig. S6A; compare Fig. 1E and Fig. 2B), in agreement with higher-level clustering analysis and with our tissue dissections (figs. S7 and S8D and tables S1 and S2). These superclusters correspond to defined anatomical regions: the medial and dorsomedial cortices, the anterior and posterior dorsal cortex, the pallial thickening, the anterior and posterior lateral cortex, and the anterior and posterior DVR (fig. S8, A to C). Cell-type similarity was generally higher within than between superclusters (fig. S8, F and G). Weighted gene correlation network analysis (WGCNA, see methods) indicates that the unique genetic signature of each region results from different combinations of gene modules (Fig. 2C). We also associated glutamatergic clusters to anatomically defined pallial regions in lizard (fig. S9). Corresponding regions in lizard and turtle have different relative sizes (for example, lizard anterior dorsal cortex is small) but are clearly delineated by the expression of the same developmental transcription factors such as *ZBTB20*, *SATB1*, *DACH2*, and *ETV1* (*ER81*) (Fig. 2D). These data define the molecular regionalization of the adult reptilian pallium.

Putative homologies between reptilian and mammalian pallial derivatives are disputed (*1*, *2*, *10*, *11*). Central to this debate is the anterior DVR, one of the derivatives of the ventral pallium, which is enlarged in birds and reptiles. This region has been proposed as a homolog of either ventral pallium derivatives [claustrum, endopiriform nucleus, and pallial amygdala (*1*, *2*, *12*)] or parts of the neocortex in mammals (*5*, *10*, *11*). The latter hypothesis suggests a dual evolutionary origin of the neocortex, either as separate regions—where medial and lateral neocortex are homologous to reptilian dorsal cortex and DVR, respectively (*11*)—or as intermixed cell types, where separate neocortical layers are homologous to reptilian dorsal cortex or DVR (*5*, *10*). We compared the turtle superclusters

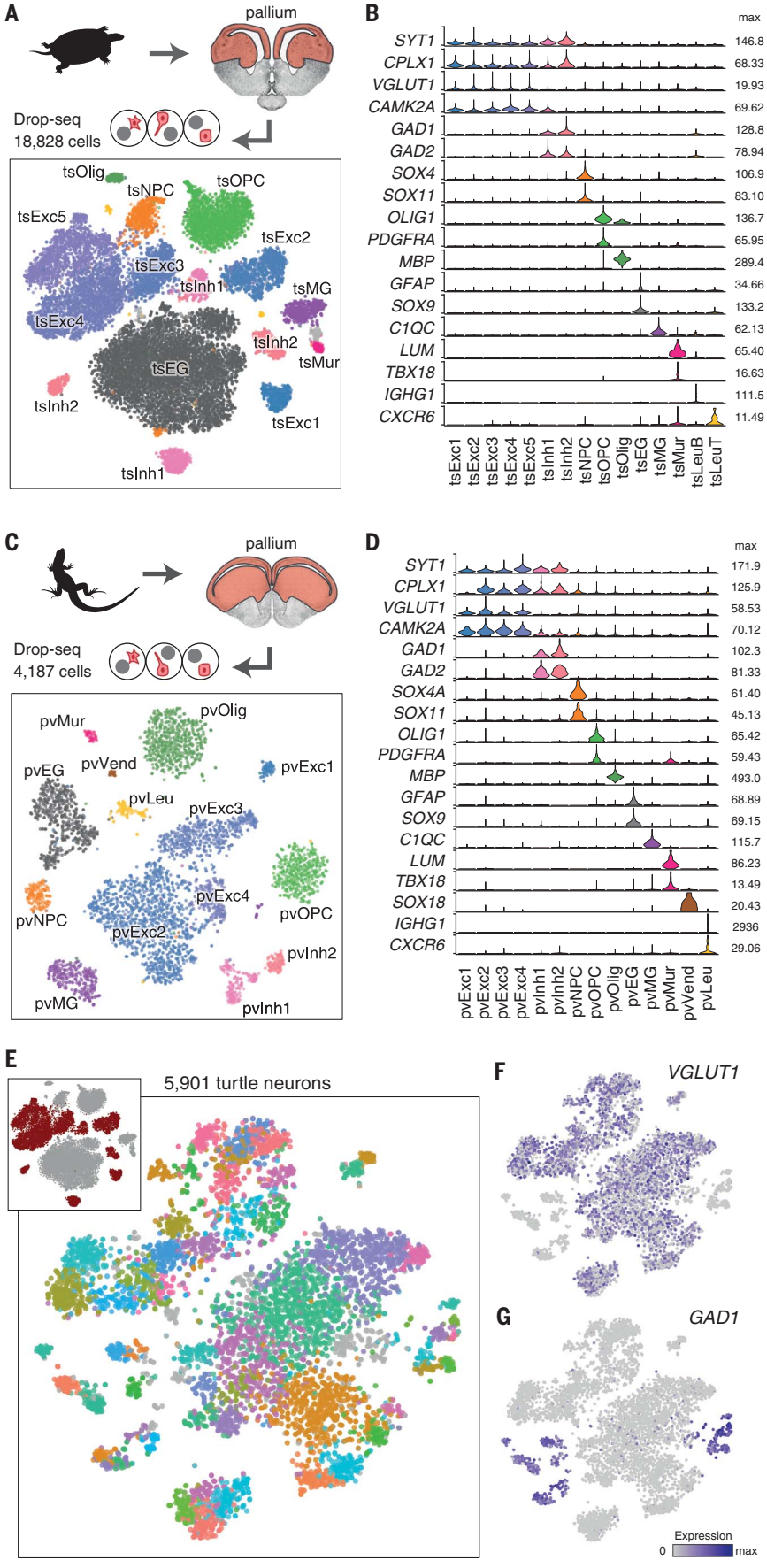

to mammalian pallial derivatives, using a human microarray data set as a reference [(*13*); see analysis in methods].

Our analysis using all differentially expressed genes (Fig. 2E) reveals similarities between turtle medial and dorsomedial cortices and human hippocampus, supporting previous hypotheses (*3*). The posterior dorsal cortex also showed positive correlations to human hippocampus and subiculum but low negative correlations with nonhippocampal cortices, consistent with the gene network analysis (Fig. 2C). Earlier studies recognized anatomical similarities between parts of the reptilian dorsal cortex and mammalian subiculum (*2*, *14*), where *ETV1* (*ER81*) is expressed (*15*). It may thus be that the posterior dorsal cortex relates to mammalian peri-hippocampal regions.

Turtle pallial thickening and mammalian claustrum shared expression of several claustrum-enriched markers (fig. S6B), consistent with anatomical and developmental data (*1*, *2*). We also found correlations between reptilian lateral cortex and mammalian piriform cortex and between posterior DVR and pallium-derived amygdalar nuclei, with the exception of the lateral amygdala. Individual posterior DVR clusters expressed markers of mammalian basolateral (*ETV1* and *FEZF2*) and cortical (*ZIC2* and *TBR1*) amygdala. These clusters mapped to distinct nuclei of the turtle posterior DVR, suggesting that these pallial amygdala subdivisions existed in the common ancestor of mammals and reptiles (fig. S10) (*16*).

Mammalian neocortex showed correlations with several turtle pallial regions (Fig. 2E). Reasoning that correlations based on all differentially expressed genes might not separate homology

Fig. 1. Reptilian single-cell data sets. (**A**) tSNE representation of 18,828 turtle (*Trachemys scripta elegans*, ts) single-cell transcriptomes, with cells color coded by cluster. (**B**) Violin plots showing expression of neuronal and non-neuronal markers in turtle clusters. (**C**) tSNE representation of 4187 lizard (*Pogona vitticeps*, pv) single-cell transcriptomes, color coded by cluster. (**D**) Violin plots showing expression of neuronal and non-neuronal markers in lizard clusters. In (B) and (D), for each gene, violin plots are scaled to the maximum number of transcripts (unique molecule identifiers) detected for that gene (max). Exc, glutamatergic excitatory neurons; Inh, GABAergic inhibitory interneurons; NPC, neural progenitor cells; Olig, mature oligodendrocytes; OPC, oligodendrocyte precursors; EG, ependymoglial cells; MG, microglia; Leu, leucocytes; Mur, mural cells; Vend, vascular endothelial cells. Subclusters of Exc and Inh cells in (A) and (C) are not matched by name or color. (**E**) tSNE plot and clusters of 5901 high-quality turtle neurons. Inset is the tSNE plot in (A), indicating neuronal and glial clusters in dark red and gray, respectively. (**F** and **G**) Expression of the glutamatergic marker *VGLUT1* (F) and GABAergic marker *GAD1* (G) in turtle neurons.

from convergent evolution (because functional convergence could recruit the same effector genes under different transcription factors), we next restricted our analysis to transcription factors. Under these conditions, only anterior dorsal cortex correlated with human neocortex (Fig. 2F). Anterior dorsal cortex and anterior DVR differed by the expression of those transcription factors that, in mammals, are also found in either the neocortex or pallial amygdala (for example, *NFIX*, *BCL11A*, and *SATB2* in turtle anterior dorsal cortex and mouse neocortex; *NR2F2* and *DACH2* in turtle anterior DVR and mouse amygdala) (fig. S8, H and I). Of the mammalian pallial amygdala subdivisions, only the lateral amygdala correlates with the anterior DVR. Our results suggest that (i) different combinations of transcription factors may regulate the expression of "neocortical" effector genes in anterior dorsal cortex and anterior DVR and (ii) transcription-factor expression reflects the developmental (and evolutionary) history of pallial neurons. We propose that reptilian anterior dorsal cortex and mammalian neocortex are homologous as dorsal pallium derivatives and that reptilian DVR and mammalian pallial amygdala are homologous as ventral pallium derivatives [see also (*1*)]. In reptiles, the expansion of the sensory-recipient anterior DVR led to the emergence of neuronal types specialized in processing different sensory modalities, recognizable as separate molecular, anatomical, and functional clusters (figs. S9 and S10) (*17*). According to this hypothesis, reptilian anterior DVR and mammalian neocortex acquired, by convergent evolution, the expression of similar sets of effector genes.

Conservation of hippocampal neuronal types and areal organization

Anatomical and developmental evidence suggest that the reptilian medial-most cortex is homologous to mammalian hippocampus (*3*, *18*). In line with this, turtle and lizard medial cortices express the mammalian pan-hippocampal transcription factor *ZBTB20* (Fig. 3A and fig. S11). Whether individual hippocampal subfields [dentate gyrus (DG), cornu ammonis (CA)3, CA2, and CA1] are present in reptiles and birds is less clear. Developmental evidence suggests so (*18*), but some describe mammalian DG, with its mossy cells and granule cells, as a mammalian novelty (*3*).

Reptilian *ZBTB20*-positive clusters could be further distinguished by the expression of mammalian DG or CA transcription factors: In turtle, *PROX1* and *MEF2C* (specifying mouse DG granule cells) labeled the medial cortex, and *ETV1*, *MEIS2*, and *LMO4* (CA) labeled the dorsomedial cortex (Fig. 3A). The expression of these genes in adjacent domains of turtle and lizard medial cortices (fig. S11) suggests the existence of DG- and CA-like neuronal types in reptiles. This was further supported by unbiased analyses of cell-type transcriptomes. Using WGCNA to identify and compare gene modules [mouse data from (*19*), see methods], we found statistically significant overlaps between mouse DG and turtle medial cortex modules and between mouse CA and turtle dorsomedial cortex modules (fig. S12). Mouse DG and turtle medial cortex modules shared genes coding for K^+-channel subunits or associated proteins (*KCNG1*, *KCNA1*, and *KCNIP4*), possibly accounting for electrophysiological similarities (*20*). Other shared genes included the cadherin *CDH8*, involved in the formation of DG-CA3 synapses, and the granule-cell specific regulators of synaptogenesis and AMPA receptor–mediated synaptic transmission *LRRTM4* and *CNIH3* (fig. S12). Hence, DG granule cells, including aspects of their membrane and synaptic physiology, are conserved across mammals and reptiles (*20*). [No mossy-cell marker (*21*) had cell-type specific expression in turtle medial cortex.]

Next, we computed pairwise cluster correlations using one-to-one orthologs differentially expressed among the *ZBTB20*$^+$ clusters. This revealed further heterogeneity among the *ZBTB20*$^+$ *ETV1*$^+$ cells, with turtle dorsomedial cortex clusters showing best mutual correlations to mouse CA3 or CA1 (Fig. 3B). Mammalian CA3 or CA1 markers (*19*, *21*) were differentially expressed in these turtle clusters (Fig. 3C). CA3- and CA1-like cells occupy adjacent positions [with CA3-like cells closest to medial cortex (DG)] and form morphologically distinct cell plates (Fig. 3A and fig. S11). We found no evidence for a reptilian CA2 cell type (Fig. 3B and fig. S11B).

In summary, reptilian hippocampus can be subdivided into adjacent territories similar to the mammalian DG, CA3, and CA1 fields. The developmental origin of these cells from the medial pallium (*18*) and their similar mediolateral distribution, connections (*22*), biophysical properties (*20*), and molecular identities (this study) support the hypothesis that mammalian-like hippocampal regions were already present as adjacent fields in the ancestor of all amniotes. The architecture of the mammalian hippocampus, with its signature infoldings, may thus result from the considerable enlargement of neocortex in the mammalian lineage.

Transcriptomic signatures of neocortical upper and deep layers in turtle dorsal cortex

Mammalian six-layered neocortex evolved from a presumed three-layered ancestral cortex in a stem amniote. What is the relationship between the neurons and layers in the mammalian neocortex and the reptilian cortex? Earlier studies suggested that L2/3 and L4 ("upper layer," UL) neurons are mammalian novelties; reptilian pyramidal neurons have thus been compared to the mammalian early born L5 and L6 ("deep layer," DL) neurons (*23*, *24*). By contrast, connectivity implies that reptilian cortex should harbor both L4 (that is, thalamorecipient) and L5 (cortico-fugal) types, and it has been suggested that these types, rather than occupying different layers, populate adjacent fields in turtle cortex: one in anterior dorsal cortex (*RORB*$^+$ L4-like neurons) and one in posterior dorsal cortex (*ETV1*$^+$ L5-like neurons) (*5*, *10*).

Our data indicate that anterior dorsal cortex is the only region comparable to mammalian neocortex (Fig. 2). We examined the expression of prototypical mammalian-layer markers (*7*, *25*, *26*) in the six turtle anterior dorsal cortex glutamatergic clusters (e07, e08, and e13 to e16). These cells expressed several mammalian UL and DL markers, but these genes were often coexpressed in the same clusters (Fig. 4A and fig. S13A). When we focused on the transcription factors that establish and maintain cell identity in the neocortex, we observed that, in the turtle, these genes were expressed in combinations that were never observed in differentiated mammalian cortical neurons. For example, all turtle anterior dorsal cortex cell types coexpress genes enriched in mammalian L2/3, L4, and L5a intratelencephalic neurons, including *SATB2*, *RORB*, and *RFX3*, as well as genes specifying L5b and L6 corticofugal projection neurons, such as *BCL11B* (*CTIP2*), *TBR1*, and *SOX5* (all clusters except e13) (*25*) (Fig. 4, A and B). In mouse neocortex, some of these genes are known to repress each other's expression in postmitotic cells (for example, *Satb2* and *Bcl11b*; *Tbr1* and *Bcl11b*) (*26*).

Extending the comparative analysis to all differentially expressed genes revealed that anterior dorsal cortex cell types correlated with either mammalian UL (e13 to e16) or DL (e07 and e08) neurons, independent of the neocortical area used for comparison (Fig. 4C and fig. S14, A to C). This trend was confirmed by gene network analysis (fig. S13, B and C). By contrast, anterior DVR clusters could not be grouped into UL- and DL-like classes (fig. S14, D to F).

As anticipated by the sequencing data, in situ hybridizations (ISHs) showed coexpression of mammalian UL and DL transcription factors throughout the turtle anterior dorsal cortex (Fig. 4B). Individual UL-like neuronal types (e13 to e16) were differentially distributed along the mediolateral and rostrocaudal axes of the anterior dorsal cortex, matching known anatomical subdivisions (fig. S15). By contrast, the DL-like cells e07 and e08, identified by parathyroid hormone–like hormone (*PTHLH*) expression, appeared interspersed throughout the anterior dorsal cortex. In the rostro-lateral dorsal cortex, DL-like cells were confined to the superficial part of L2 (Fig. 4D; additional markers in fig. S15, C to E). These markers thus identify two distinct sublayers in turtle L2: a superficial L2a with mostly DL-like neurons and a deeper L2b with mostly UL-like neurons. Retrograde tracing from the thalamus labels L2a cells (*27*, *28*), suggesting that these neurons, or a subset of them, are corticofugal and project to the thalamus.

In conclusion, our transcriptome-wide comparisons reveal the presence of global UL- and DL-like genetic signatures in distinct neuronal types of turtle anterior dorsal cortex but do not support, with the current resolution, homologies between turtle glutamatergic types and individual neocortical layers. In reptiles and mammals, UL and DL genetic signatures might have evolved independently from a stem amniote that lacked distinct UL- and DL-like neurons: Neurons with similar characteristics, such as input-output connectivity, would have acquired the

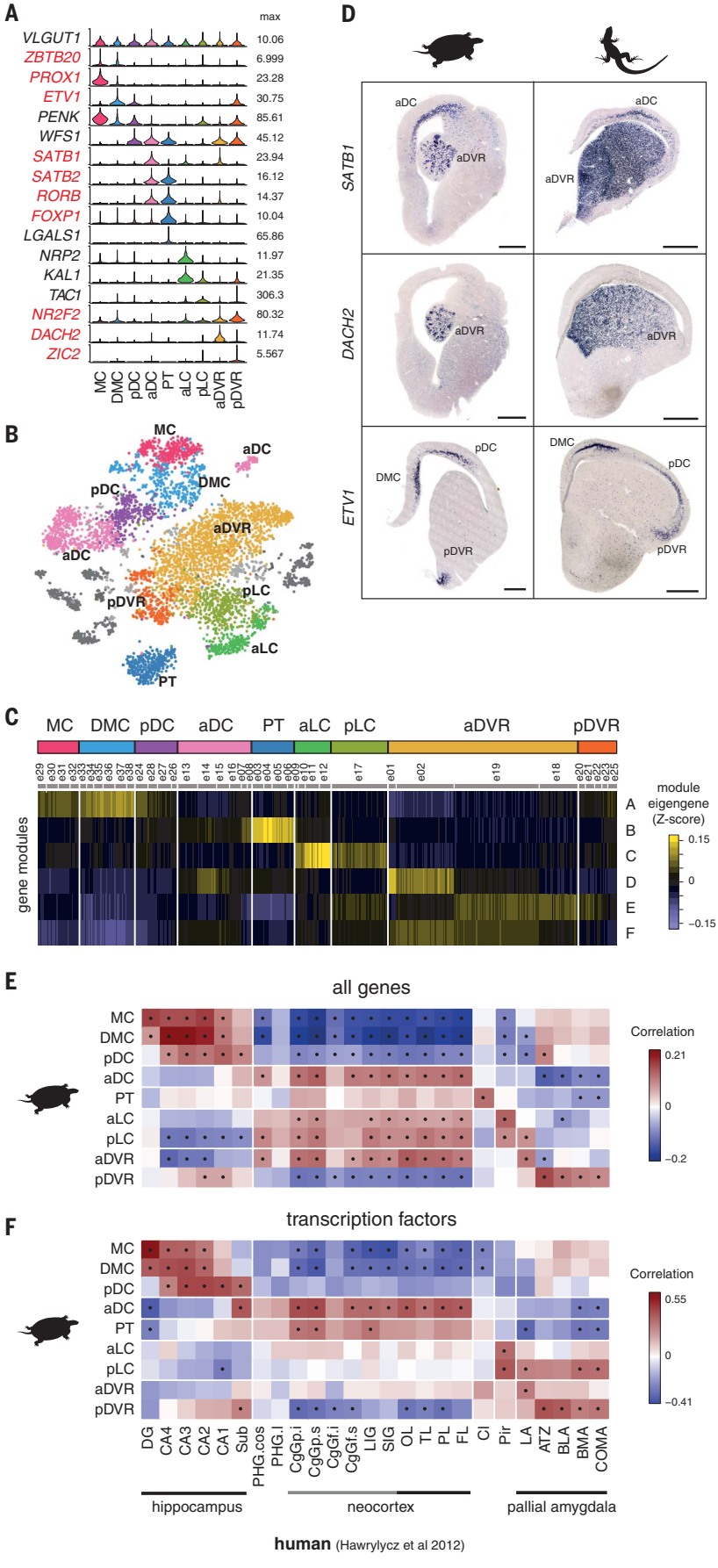

expression of similar gene sets by convergent evolution. Alternatively, UL- and DL-like neurons may have existed already in the dorsal cortex of stem amniotes. If true, the emergence of the six layers that form mammalian neocortex would be a novelty [sensu (*29*)], with the evolution of new pyramidal cell types through extensive modifications of the genetic programs specifying ancestral UL- and DL-like types.

Conservation of GABAergic interneuron classes across amniotes

GABAergic interneurons in mammalian neocortex are diverse and participate in different circuit motifs and computations (*30*). Little is known about cortical interneurons outside of mammals. In several vertebrates, including reptiles, GABAergic interneurons are generated in conserved subpallial regions—the medial, caudal, and lateral ganglionic eminences (MGE, CGE, and LGE)—and migrate to the pallium (*31*, *32*). Reptiles, however, are thought to lack some mammalian GABAergic types, such as cortical vasoactive intestinal peptide (VIP) interneurons (*24*). We examined the turtle GABAergic clusters (i01 to i18) and the expression of transcription factors known to define mammalian GABAergic types.

Fig. 2. Reptilian pallial regions. (**A**) Violin plots showing expression of genes discriminating between spatially segregated glutamatergic neurons in the turtle pallium. (**B**) tSNE showing turtle glutamatergic neurons colored by supercluster. Transcription factor names are in red. (**C**) Heatmap showing expression of module eigengenes calculated from turtle glutamatergic neurons. Pseudocells (averages of 4 to 5 cells used for WGCNA, see methods) are shown in columns, ordered by cluster and supercluster. (**D**) Expression of transcription factors that label corresponding pallial regions in turtle and lizard (ISH, frontal sections at different anterior-posterior levels; see also figs. S8 and S9). Scale bars, 1 mm. (**E** and **F**) Pairwise correlations of turtle glutamatergic superclusters and human pallial regions, calculated from all genes (E) or transcription factors (F) differentially expressed in turtle or human. In mammals, only some parts of the cingulate gyrus (CgG), long insular gyrus (LIG), and short insular gyrus (SIG) are classified as neocortex [see (*13*) for human data]. Dots indicate statistically significant correlations. MC, medial cortex; DMC, dorsomedial cortex; pDC and aDC, posterior and anterior dorsal cortex; PT, pallial thickening; aLC and pLC, anterior and posterior lateral cortex; aDVR and pDVR, anterior and posterior dorsal ventricular ridge; DG, dentate gyrus; CA, cornu ammonis; Sub, subiculum; PHG, parahippocampal gyrus; OL, occipital lobe; TL, temporal lobe; PL, parietal lobe; FL, frontal lobe; Cl, claustrum; Pir, piriform cortex; LA, lateral amygdala; ATZ, amygdalohippocampal transition zone; BLA, basolateral amygdala; BMA, basomedial amygdala; COMA, corticomedial amygdala.

From the combinatorial expression of these genes, we identified putative MGE-derived (i07 to i13: *LHX6*$^+$, *SOX6*$^+$, and *SATB1*$^+$), CGE-derived (i14 to i18: *NPAS1*$^+$, *SP8*$^+$, *NR2E1*$^+$, and *PROX1*$^+$), and LGE-derived (i01 and i04 to i06: *MEIS2*$^+$ *ZIC1*$^-$ and in subsets *TSHZ1*$^+$ *SIX3*$^+$ and/or *PBX3*$^+$) clusters (Fig. 5A). Corresponding MGE-, CGE-, and LGE-derived neurons could also be identified in lizard (fig. S16, A to C). The remaining GABAergic clusters correspond to cells dissected from the neighboring septum (i02 and i03) and striatum (i04). Stainings revealed the presence of LGE- and septum-derived interneurons in the amygdala (i04 and i05) and olfactory bulb (i01 and i02), indicating that LGE- and septum-derived GABAergic neurons have similar molecular identities and migratory trajectories in reptiles and mammals (Fig. 5A and fig. S16, D and E).

Turtle MGE- and CGE-derived interneurons could be further subdivided into somatostatin ("SST"), parvalbumin-like ("PV-like"), "HTR3A Reln," and "HTR3A VIP-like" classes, matching the classification of mammalian cortical GABAergic interneurons (*7*, *30*) (Fig. 5A). Pairwise cluster correlations (Fig. 5B) and gene network analysis (fig. S17) further supported the conclusion that PV-like, SST, and HTR3A interneuron classes are conserved in reptiles and mammals. [Note that transcriptomics identifies VIP- and PV-like interneurons even though *VIP* and *PVALB* are not reliably expressed in these cells (Fig. 5A).]

In turtle and lizard, markers of MGE- and CGE-derived interneurons were expressed in cells scattered throughout the pallium, including the dorsal cortex (Fig. 5C). As in mammals, where MGE- and CGE-derived interneurons have different densities across cortical layers, neurons expressing *ADARB2* (HTR3A) and *SST* (SST) were found preferentially in superficial and deep dorsal cortex, respectively; *NDNF* (HTR3A Reln) was expressed in rare dorsal cortex subpial cells, reminiscent of mammalian L1 neurogliaform cells (Fig. 5, D and E). Because the same classes of cortical GABAergic neurons exist in mammals and reptiles, they likely existed in their amniote ancestor. Our analysis did not detect similarities at a finer level: For example, we found no turtle

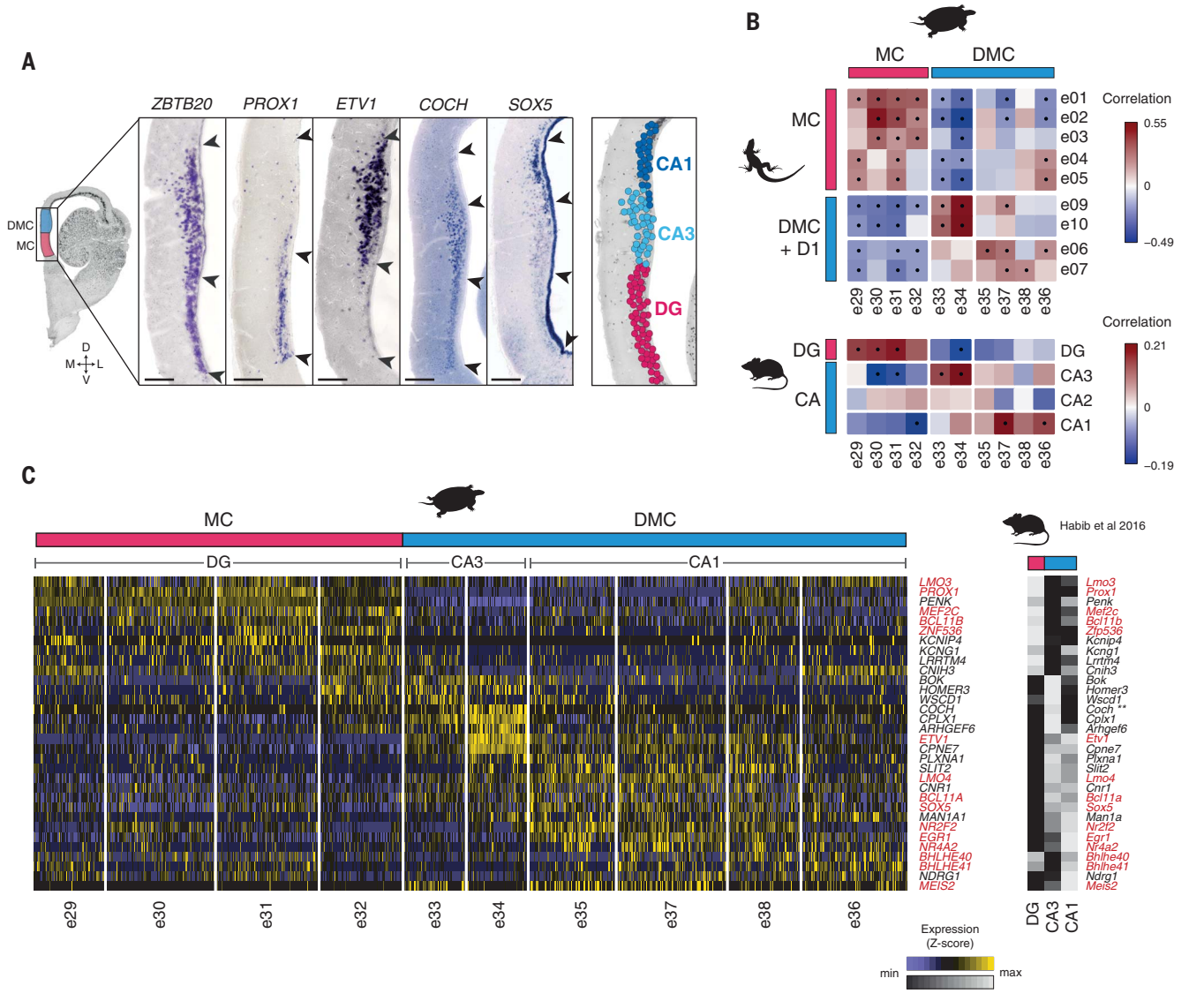

Fig. 3. Molecular architecture of the reptilian hippocampus. (**A**) Expression of hippocampal markers in turtle medial (MC) and dorsomedial (DMC) cortices. Arrowheads indicate boundaries between DG, CA3, and CA1 (compare to schematic at right). D, dorsal; V, ventral; M, medial; L, lateral. (**B**) Pairwise correlations of turtle and lizard (top) and turtle and mouse (bottom) hippocampal clusters. Dots indicate statistically significant correlations. In lizard, the *ZBTB20*$^+$ *ETV1*$^+$ medial cortices are termed DMC and D1 in the classical literature but correspond to turtle DMC. (**C**) On the left, expression of mammalian hippocampal markers in turtle single cells (columns, arranged by cluster) and, on the right, expression of the same markers in mouse [data from (*19*)]. Transcription factor names are in red. Scale bars, 200 μm.

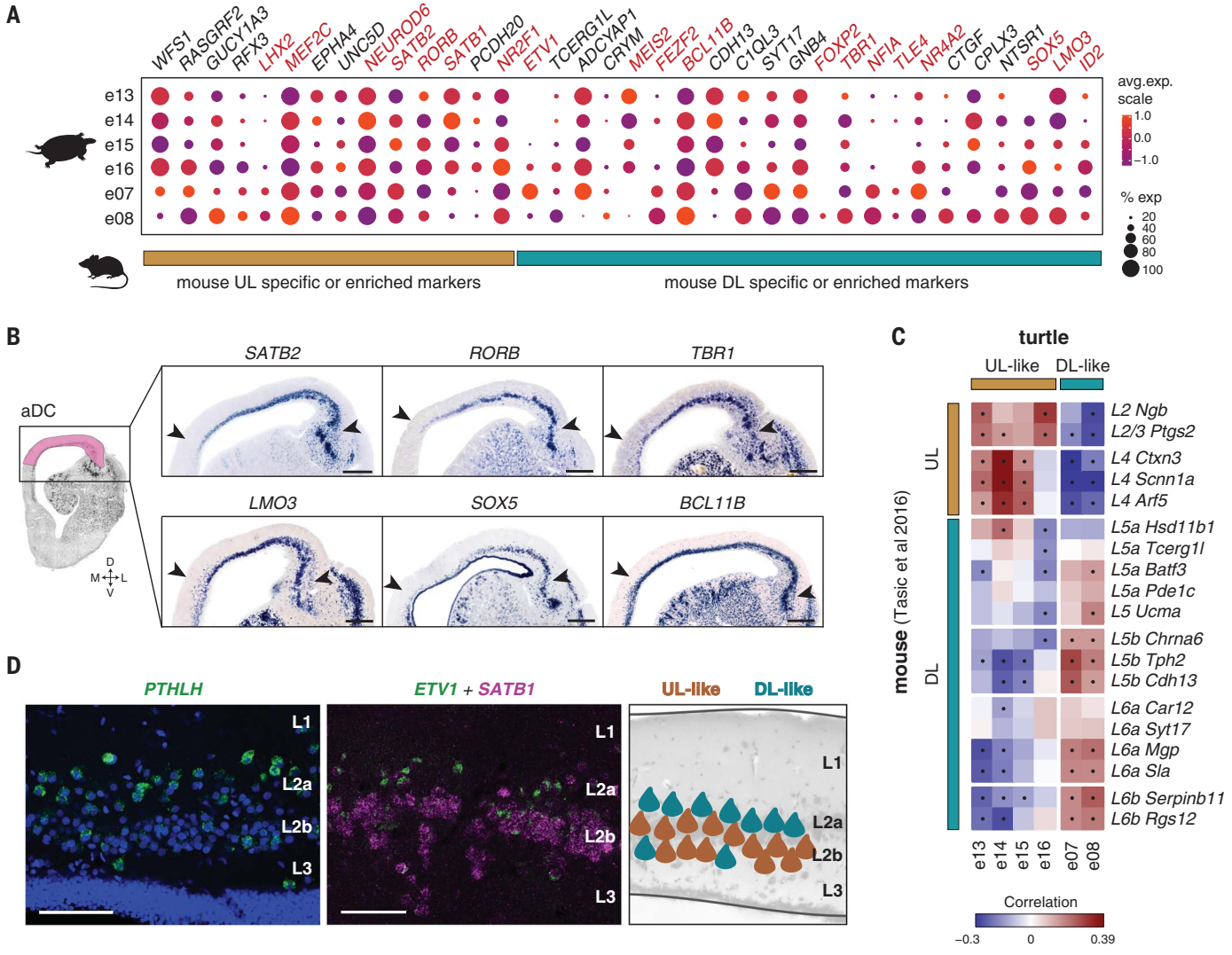

Fig. 4. UL- and DL-like neurons in turtle dorsal cortex. (**A**) Dot-plot showing expression of canonical mammalian layer markers (columns) in turtle anterior dorsal cortex (aDC) clusters (rows). Dot size indicates the percentage of cells in the cluster where the gene is detected; color indicates expression (exp) level. Names of transcription factors are in red. (**B**) ISHs showing expression of mammalian UL and DL transcription factors throughout the turtle aDC. Arrowheads indicate the medial and lateral boundaries of anterior dorsal cortex. Scale bar, 500 μm. (**C**) Pairwise correlations of turtle aDC (columns) and mouse neocortex (rows) glutamatergic types. Dots indicate statistically significant correlations. Mouse clusters are from (*7*). (**D**) Left panel, turtle DL-like cells, labeled by *PTHLH* (green), are preferentially found in superficial L2 [blue, 4′, 6-diamidino-2-phenylindole (DAPI)]. Middle panel, double ISH for *SATB1* (enriched in UL-like cells, magenta) and *ETV1* (e07 DL-like cells, green), showing the relative positions of these cells. Right panel, schematic summarizing the distribution of UL- and DL-like glutamatergic neurons (inverse arrangement to that observed in mammals). See also fig. S15. Scale bar, 100 μm.

clusters corresponding to mammalian Martinotti or basket cells. This suggests that species-specific subtypes of interneurons diversified independently in mammals and reptiles from ancestral PV-like, SST, and HTR3A (possibly VIP-like and Reln) cell classes.

Discussion

Our single-cell data provide molecular support to the existence of conserved regions and cell types in the amniote pallium. Homologs of the mammalian neocortex, "core" hippocampus (with dentate and CA fields), claustrum, and pallial amygdala probably existed already in stem amniotes. Glutamatergic neurons with an UL- or DL-like genetic signature exist in turtle anterior dorsal cortex, but one-to-one homologies of these cell types and individual mammalian layer types are not supported by our data. By contrast, cortical GABAergic interneuron classes (SST, PV-like, and HTR3A) are ancestral in amniotes.

Our analysis indicates that mammalian and reptilian brains diversified by expansion and independent evolution of different pallial territories and that these expansions coincided with the evolution of new neuronal types. The large reptilian anterior DVR (ventral pallium), for example, consists of spatially segregated neuronal types specialized in processing visual, auditory, or somatosensory stimuli (*17*). The same sensory pathways also reach the ventral pallium of mammals (for example, the lateral amygdala) but are not processed by dedicated neuronal populations there (*12*). This suggests that the elaboration of DVR neurons and circuits is specific to reptiles and birds.

The situation is reversed with the dorsal pallium. Mammalian neocortex emerged by expansion of a small dorsal pallial territory, homologous to the anterior dorsal cortex of reptiles and to the avian Wulst (*1*). This may have coincided with the generation of new glutamatergic cell types from the diversification of UL- and DL-like neurons. The sequential generation of neurons with distinct identities is a conserved feature of mammalian and reptilian (*33*) dorsal pallium progenitors, and corticothalamic neurons are early born neurons in mouse and turtle (*28*).

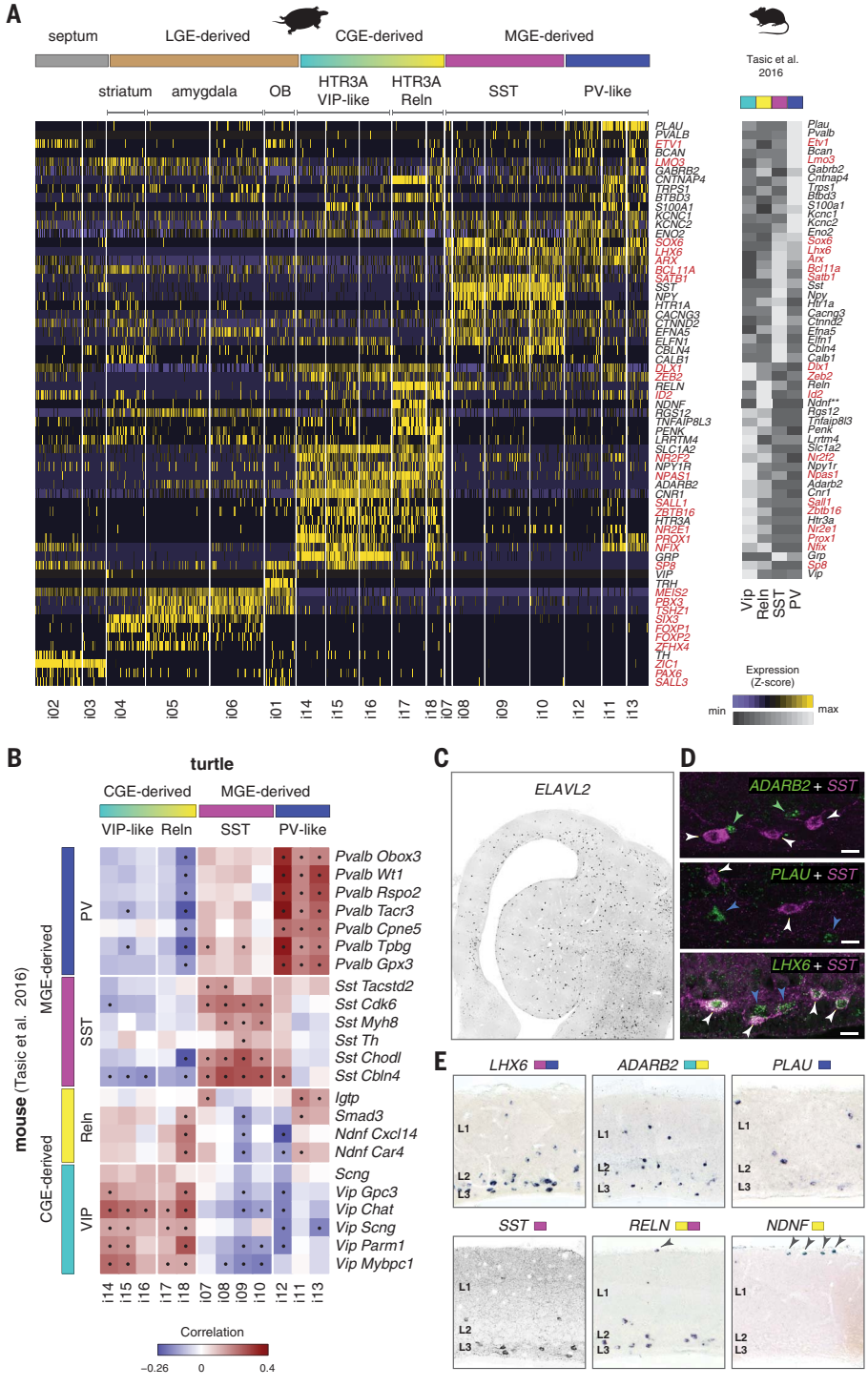

Fig. 5. Turtle GABAergic interneurons. (**A**) On left, heatmap showing expression of selected mammalian GABAergic markers (rows) in turtle single cells, grouped by cluster (column), and, on right, expression of the same markers in mouse cortical GABAergic cells [data from (*7*)]. Names of transcription factors are in red. OB, olfactory bulb. (**B**) Pairwise correlations of turtle (columns) and mouse (rows) MGE- and CGE-derived GABAergic clusters. Dots indicate statistically significant correlations. (**C**) GABAergic neurons, labeled by *ELAVL2*, in turtle. (**D**) Double labeling of *SST* (immunohistochemistry, magenta) and *ADARB2*, *PLAU*, or *LHX6* (ISH, green) in turtle dorsal cortex. *LHX6* labels both SST^+ (SST) and SST^- (PV-like) neurons. White arrowheads indicate SST neurons (SST^+ $LHX6^+$); blue arrowheads indicate PV-like neurons ($PLAU^+$ $LHX6^+$ SST^-); green arrowheads indicate HTR3A neurons ($ADARB2^+$). Scale bars, 20 μm. (**E**) ISHs of GABAergic markers in turtle dorsal cortex.

Neuronal birth order is the same in turtle and mammals (DL first, UL late) (*28*), and the superficial position of turtle DL-like neurons is consistent with the inversion of corticogenesis (outside-in in reptiles, inside-out in mammals) (*28*, *34*). Finally, in mammals, transcription factors specifying UL and DL fate are coexpressed in progenitors and acquire mutually exclusive expression only after cell-cycle exit (*35*). The coexpression of mammalian UL and DL fate specifiers in turtle neurons suggests that cortical layers may have evolved from the remodeling of regulatory interactions between these transcription factors, possibly through new repressive interactions. The temporal extension of neurogenesis (*33*) could have enabled the segregation of originally overlapping gene expression programs and thus the diversification of ancestral UL and DL types.

These molecular maps of turtle and lizard pallium provide a framework for future functional studies. How do similarities and differences in gene expression programs inform us about the evolution of brain function? Much of reptilian cortex, for example, is molecularly related to core mammalian hippocampus. Lesion experiments in reptiles suggest a role for medial cortex in navigation (*22*), but no chronic electrophysiological data have, as of yet, been obtained from these regions. Integrating our molecular maps with tracing, electron microscopy, and electrophysiological studies is needed to understand whether and how gene expression programs are linked to the evolution of connectivity and function.

Common principles of synaptic organization can be extrapolated from the comparison of three- and six-layered cortices (*36*). Are these similarities coincidental or do they reflect ancestral cortical circuits? In mammals, local circuit motifs involve GABAergic types with distinct molecular and functional features (*30*). Our study indicates that interneuron diversity is ancestral to both mammals and reptiles. The conservation of interneuron classes over at least 320 million years suggests not only that there is selective pressure for interneuron diversity but also that interneuron diversity itself may have evolved in stem vertebrates within primordial cortical circuits (*37*). Alternatively, the conservation of interneuron classes may result simply from developmental constraints on subpallium patterning. The combined molecular and functional investigation of circuit motifs in reptilian cortex may shed light on the ancestral design and computational logic of vertebrate cortices.

REFERENCES AND NOTES

1. L. Puelles *et al.*, in *Evolution of Nervous Systems*, J. H. Kaas, Ed. (Elsevier, ed. 2, 2017), vol. 1, pp. 519–555.
2. G. F. Striedter, *Brain Behav. Evol.* **49**, 179–194 (1997).
3. G. F. Striedter, *J. Comp. Neurol.* **524**, 496–517 (2016).
4. T. G. Belgard *et al.*, *Proc. Natl. Acad. Sci. U.S.A.* **110**, 13150–13155 (2013).
5. J. Dugas-Ford, J. J. Rowell, C. W. Ragsdale, *Proc. Natl. Acad. Sci. U.S.A.* **109**, 16974–16979 (2012).
6. A. Zeisel *et al.*, *Science* **347**, 1138–1142 (2015).
7. B. Tasic *et al.*, *Nat. Neurosci.* **19**, 335–346 (2016).

8. E. Z. Macosko *et al*., *Cell* **161**, 1202–1214 (2015).
9. G. La Manno *et al*., *Cell* **167**, 566–580.e19 (2016).
10. H. J. Karten, *Curr. Biol.* **23**, R12–R15 (2013).
11. A. B. Butler, Z. Molnár, *Brain Res. Bull.* **57**, 475–479 (2002).
12. L. L. Bruce, T. J. Neary, *Brain Behav. Evol.* **46**, 224–234 (1995).
13. M. Hawrylycz *et al*., *Nat. Neurosci.* **18**, 1832–1844 (2015).
14. P. V. Hoogland, E. Vermeulen-Vanderzee, *J. Comp. Neurol.* **285**, 289–303 (1989).
15. H. Yoneshima *et al*., *Neuroscience* **137**, 401–412 (2006).
16. N. Moreno, A. González, *J. Anat.* **211**, 151–163 (2007).
17. P. R. Manger, D. A. Slutsky, Z. Molnár, *J. Comp. Neurol.* **453**, 226–246 (2002).
18. L. Medina, A. Abellán, E. Desfilis, *Brain. Behav. Evol.* **90**, 25–40 (2017).
19. N. Habib *et al*., *Science* **353**, 925–928 (2016).
20. J. M. Shen, A. R. Kriegstein, *J. Neurophysiol.* **56**, 1626–1649 (1986).
21. M. S. Cembrowski, L. Wang, K. Sugino, B. C. Shields, N. Spruston, *eLife* **5**, e14997 (2016).
22. S. Reiter, H.-P. Liaw, T. M. Yamawaki, R. K. Naumann, G. Laurent, *Brain. Behav. Evol.* **90**, 41–52 (2017).
23. F. F. Ebner, in *Evolution of Brain and Behavior in Vertebrates*, R. B. Masterton, M. E. Bitterman, C. B. G. Campbell, N. Hotton, Eds. (Lawrence Erlbaum Associates, Hillsdale, NJ, 1976), pp. 115–167.
24. A. Reiner, *Comp. Biochem. Physiol. Comp. Physiol.* **104**, 735–748 (1993).
25. B. J. Molyneaux, P. Arlotta, J. R. L. Menezes, J. D. Macklis, *Nat. Rev. Neurosci.* **8**, 427–437 (2007).
26. L. T. Gray *et al*., *eLife* **6**, 1–30 (2017).
27. P. S. Ulinski, *J. Comp. Neurol.* **254**, 529–542 (1986).
28. M. G. Blanton, A. R. Kriegstein, *J. Comp. Neurol.* **310**, 558–570 (1991).
29. D. Arendt *et al*., *Nat. Rev. Genet.* **17**, 744–757 (2016).
30. R. Tremblay, S. Lee, B. Rudy, *Neuron* **91**, 260–292 (2016).
31. C. Métin *et al*., *Development* **134**, 2815–2827 (2007).
32. O. Marín, J. L. R. Rubenstein, *Nat. Rev. Neurosci.* **2**, 780–790 (2001).
33. T. Nomura, H. Gotoh, K. Ono, *Nat. Commun.* **4**, 2206 (2013).
34. A. M. Goffinet, C. Daumerie, B. Langerwerf, C. Pieau, *J. Comp. Neurol.* **243**, 106–116 (1986).
35. S. Lodato, P. Arlotta, *Annu. Rev. Cell Dev. Biol.* **31**, 699–720 (2015).
36. G. M. Shepherd, *Front. Neuroanat.* **5**, 30 (2011).
37. S. M. Suryanarayana, B. Robertson, P. Wallén, S. Grillner, *Curr. Biol.* **27**, 3264–3277.e5 (2017).

ACKNOWLEDGMENTS

The authors are grateful to V. Benes and P. Collier (EMBL GeneCore Facility, Heidelberg) for training and support on sequencing; A. Georges (University of Canberra) for prepublication access to the *Pogona* genome; C. Müller (MPI for Brain Research) for initial investigations on turtle GABAergic interneurons; M. Klinkmann, A. Arends, A. Macias Pardo, T. Manthey, C. Thum, and J. Knop for technical assistance; S. Masneri for help with scientific computing; and E. Schuman, C. Müller, S. Reiter, and the Laurent laboratory for feedback during the course of this work and on the manuscript.

Funding: This research was funded by the Max Planck Society and the European Research Council under the European Union's Seventh Framework Programme (FP7/2007-2013)/ERC grant agreement n° 322705 (G.L.). **Author contributions:** Single-cell experiments: M.A.T. and T.M.Y.; bioinformatics: M.A.T., T.M.Y., and G.T.; anatomy and histology: M.A.T., R.K.N., and A.A.J.; data analysis: M.A.T., T.M.Y., R.K.N., A.A.J., G.T., and G.L.; project management and supervision: G.L.; and manuscript writing: M.A.T. and G.L., with input from T.M.Y. and R.K.N. **Competing interests:** The authors declare no competing interests. **Data and materials availability:** Sequencing data have been deposited in the NCBI Sequence Read Archive (BioProject PRJNA408230), and processed gene expression data can be explored at https://brain.mpg.de/research/laurent-department/software-techniques.html. The code used for analysis is available at https://github.molgen.mpg.de/MPIBR/ReptilePallium/.

SUPPLEMENTARY MATERIALS

www.sciencemag.org/content/360/6391/881/suppl/DC1
Materials and Methods
Figs. S1 to S17
Tables S1 and S2
References (*38*–*55*)

6 November 2017; accepted 12 March 2018
Published online 3 May 2018
10.1126/science.aar4237